https://doi.org/10.5194/gmd-2024-168
Preprint. Discussion started: 10 October 2024

Geoscientific Model Development
Discussions
Open Access

NMP-Hydro 1.0: a C# language and Windows System based Ecohydrological Model Derived from Noah-MP

Yong-He Liu[1], Zong-Liang Yang[2]
[1] School of Resources and Environment, Henan Polytechnic University, Jiaozuo, Henan, China
[2] Jackson School of Geoscience, University of Texas at Austin, Austin TX, USA

Correspondence: Yong-He Liu (yonghe_hpu@163.com)

Abstract. The community Noah with multi-parameterization options (Noah-MP) land surface model (LSM) is widely used in studies from uncoupled land surface hydrometeorology and ecohydrology to coupled weather and climate predictions. In this study, we developed NMP-Hydro 1.0, a hydrological model written in CSharp(C#). NMP-Hydro was developed by faithfully translating the FORTRAN version Noah-MP from the uncoupled WRF-Hydro 3.0, and was coupled with a river routing model. NMP-Hydro has the capacity of execution on Windows systems, utilizing the multi-core CPUs commonly available in today's personal computers. The code of NMP-Hydro has been tested to ensure that it produces a high-degree of consistency with the output of the original WRF-Hydro. High-resolution (6 km) simulations were conducted and assessed over a grid domain covering the entire Yellow River Basin and the most part of North China. The spatial maps and temporal variations of many state variables simulated by NMP-Hydro 1.0 and WRF-Hydro/Noah-MP demonstrate consistent results, with occasionally minor discrepancies. The river discharge for the Yellow River under various scheme combinations of six Noah-MP parameterizations exhibits general agreement with the natural river discharge at the Lanzhou station. NMP-Hydro can be regarded as a reliable replica of Noah-MP in WRF-Hydro 3.0, but it can leverage the modern, powerful, and user-friendly features brought by the C # language to significantly improve the efficiency of the model users and developers.

1. Introduction.

In contemporary hydrological prediction and flood warning applications, the effectiveness of hydrological models hinges on their ability to delineate intricate energy and water processes on the land surface, surpassing the capabilities of traditional rainfall-runoff models. To address this demand, certain land surface models (LSMs) utilized by atmospheric science communities have been bolstered with hydrological simulation features, as observed in WRF-Hydro (Lin et al., 2018), or conventional rainfall-runoff models have been enriched with more comprehensive descriptions of land surface processes, exemplified by the VIC model (Liang et al., 1994).

The Noah Land Surface Model with multi-parameterizations (Noah-MP) (Niu et al., 2011; Yang et al., 2011)stands out as a robust tool for studying global water issues, serving as the foundation for models like WRF-Hydro, which incorporates Noah-MP (Gochis, 2020). However, the code for Noah-MP and WRF-Hydro is written in FORTARN, a 'legacy' language, posing challenges for code analysis and editing, unlike more modern languages such as CSharp(C#) or Java. This limitation makes it arduous for users unfamiliar with FORTRAN to comprehend and modify the code. Additionally, Noah-MP and WRF-Hydro necessitate a UNIX-like operating system, causing inconvenience for users and developers

https://doi.org/10.5194/gmd-2024-168
Preprint. Discussion started: 10 October 2024

Geoscientific Model Development Discussions

relying on Windows systems. Therefore, there is a compelling need to code Noah-MP in a contemporary modern programming language.

We designed NMP-Hydro 1.0, a hydrological model based on Noah-MP but coded using the CSharp (C#) language. This model was crafted by creating a framework and accurately translating the original Noah-MP LSM code from WRF-Hydro 3.0 and coupling with a Muskingum method-based river routing model(Liu et al., 2023). C#, recognized for its modern and object-oriented approach, is widely used for software development across various platforms, particularly on the Windows operating system.

NMP-Hydro offers several advantages over the original WRF-Hydro/Noah-MP. Unlike the original version that requires compiling for each computer and predominantly relies on Unix-like systems, NMP-Hydro can seamlessly run on Windows systems supporting the Microsoft Dotnet Framework. The executable files, once compiled, can be easily packaged and distributed to other Windows computers, providing convenience for users less familiar with Unix-like operations. The utilization of the C# language facilitates advanced software programs for code visualization and analysis, enhancing user convenience for code reading and modification. The model's design aligns with the input datasets and settings in the 'namelist' file, ensuring compatibility with WRF-Hydro 3.0. Based on the support of parallel computation of C#, both the translated Noah-MP LSM simulation and the river routing simulation in NMP-Hydro support parallel execution on common personal computers.

2 The Noah-MP LSM

Noah-MP is a robust model renowned for its capability to represent diverse physical processes. Since its initial introduction by Niu et al. （2011) and Yang et al. (2011), Noah-MP has been seamlessly integrated into the Weather Research and Forecasting (WRF) model, giving rise to the WRF-Hydro model, as elucidated by Gochis (2020). Furthermore, the offline WRF-Hydro model plays a pivotal role in the National Water Model, contributing to the simulation of floods and river flows across the United States, as highlighted by Bales (2019), Francesca et al. (2020), and Karki et al. (2021). Noah-MP's versatility extends to applications such as streamflow prediction (Lin et al., 2018) and the estimation of spatial distributions for evapotranspiration, surface temperature, carbon fluxes, heat fluxes, and soil moisture, as demonstrated in many studies (Chang et al., 2020; Gao et al., 2015; Li et al., 2022; Ma et al., 2017; Yang et al., 2021)..

Noah-MP excels in physically representing water and energy dynamics across various environmental layers, encompassing a vegetation canopy layer, multiple snow and soil layers, and an optional unconfined aquifer layer for groundwater. Unlike functioning in isolation, Noah-MP is typically coupled with host models, such as the community WRF-Hydro modelling framework (Lin et al., 2018) and HRLDAS (Chen et al., 2007), emphasizing its collaborative nature. Additionally, Noah-MP plays a pivotal role in the National Water Model (Francesca et al., 2020; Gochis, 2020), contributing to real-time streamflow forecasts for the entire United States of America. To capture specific physical processes, Noah-MP employs multiple parameterization schemes, offering users the flexibility to select from a total of 12 parametrizations, as outlined in Table 1. This versatility enables tailored representation of diverse environmental conditions and processes, enhancing the model's adaptability and applicability.

Table 1: Parameterization Options for Noah-MP (an asterisk (*) denotes the recommended default option). Certain abbreviations correspond to terms used for Parameterization Schemes (PS) in Noah-

https://doi.org/10.5194/gmd-2024-168
Preprint. Discussion started: 10 October 2024

MP, and their meanings can be referenced in the Noah-MP user document. For instance, LAI and FVEG represent the leaf area index and the fraction of vegetation cover, respectively.

Abbreviation	Physical parameterization	Scheme Code	Scheme Options
DVEG	Vegetation option	1~5	*1 table LAI, read FVEG; 2 dynamic LAI, FVEG=f(LAI); 3 table LAI, FVEG=f(LAI); 4 table LAI, FVEG=maximum; 5 dynamic LAI, FVEG =maximum
CRS	Stomatal conductance (controls transpiration from leaves)	1~2	*1 Ball-Berry; 2 Jarvis
BTR	β-factor (soil moisture stress factor controlling transpiration)	1~3	*1 Noah; 2 CLM; 3 SSiB
RUN	Runoff (runoff generation at and below the surface)	1~4	1 SIMGM; 2 SIMTOP; *3 Schaake96; 4 BATS
SFC	Surface layer drag coefficient	1~2	*1 M-O; 2 Chen97
FRZ	Frozen soil permeability	Fixed to 2	*1 NY06; 2 Koren99
INF	Supercooled liquid water	Fixed to 2	*1 NY06; 2 Koren99
RAD	Radiation transfer option	1~3	1 gap=F(3D,cosz); 2 gap=0; *3 gap=1-Fveg
ALB	Snow surface albedo	Fixed to 2	1 BATS; *2 CLASS
SNF	Precipitation partition option (rainfall or snowfall)	Fixed to 2	*1 Jordan91; 2 BATS; 3 Noah
TBOT	Lower boundary of soil temperature	1~2	*1 zero-flux; 2 Noah
STC	Snow/soil temperature time scheme	Fixed to 1	*1 semi-implicit; 2 fully implicit; 3 Ts=f(fsno)

3 Development of NMP-Hydro

3.1 Translation of Noah-MP Code

Our primary focus in developing NMP-Hydro involved translating the original FORTRAN code of Noah-MP into the C# language. The overarching objective of this translation is to create a hydrological model based on Noah-MP capable of functioning seamlessly on Windows systems. It is essential to note that this translation is based on a relatively older version of Noah-MP utilized in WRF-Hydro 3.0, as the process commenced before the release of Noah-MP 5.0 (He et al., 2023).
Converting FORTRAN code into C# is not straightforward due to significant differences in syntax between the two languages. The reconstruction of the model in the C# language follows a straightforward object-oriented design. While FORTRAN is traditionally a function-based language, the core Noah-MP module's functions, subroutines, and state variables are encapsulated as members within a class named GridCell (**Fig. 1(a)**). This class represents all Noah-MP behaviors within a grid box. The variable names, function definitions, data structures, and execution logic have been kept

https://doi.org/10.5194/gmd-2024-168
Preprint. Discussion started: 10 October 2024

Geoscientific Model Development Discussions
Open Access

largely consistent with the original FORTRAN code, ensuring user-friendliness for those familiar with Noah-MP. To handle multiple grid boxes, another class named Driver is employed. This class manages tasks such as initializing model variables, creating multiple grid boxes, reading/writing files, and controlling the execution of the model.

Throughout the translation process, a key focus was addressing operations on FORTRAN arrays (**Fig. 1(b)**), crucial for representing the state of soil and snow layers in Noah-MP. Unlike C#, FORTRAN allows arrays to have user-specified index ranges (e.g., index values from -3 to 4). However, in C#, the first index of all arrays invariably starts from 0. To streamline the translation, we introduced a new array class named FortArray, designed to mimic FORTRAN arrays. The inner array data in FortArray adheres to standard C# conventions, accepting 0 as the inner index of the first element. Yet, externally, the class allow access to the array values through extra indices. The class provides methods for index translation from outer indices to inner indices:

$$I_{in} = I_{ex} - I_{start} \quad (1)$$

Where I_{in}, I_{ex} and I_{start} represent the inner index, outer index and the first outer index. The inner index corresponds to the standard C# arrays, while the outer index corresponds to the FORTRAN arrays. For instance, if a FORTRAN array of 8 elements has an index range from -3 to 4, this array is translated into a FortArray that has a standard inner array of 8 elements and accompanied by two arguments representing the start FORTRAN index (-3) and the end FORTRAN index (4), then the range of its inner indices are 0~7. This array translation technique ensures that all the original execution logic in Noah-MP is seamlessly preserved in NMP-Hydro.

The model also supports parallel execution, implemented through the native parallel functionality of the C# language. These functions efficiently allocate computational tasks for distinct grid boxes to different CPU threads. For instance, if a specific domain requires the execution of 2400 grid boxes, and the tasks are assigned to 8 threads, each thread is responsible for completing the tasks of approximately 300 grid boxes. It's crucial to note that if the number of specified threads exceeds the actual number of CPU cores, multiple threads may end up executing on a single CPU core. Therefore, specifying more threads than the available CPU cores does not contribute to an overall improvement in execution speed.

https://doi.org/10.5194/gmd-2024-168
Preprint. Discussion started: 10 October 2024

Geoscientific Model Development Discussions

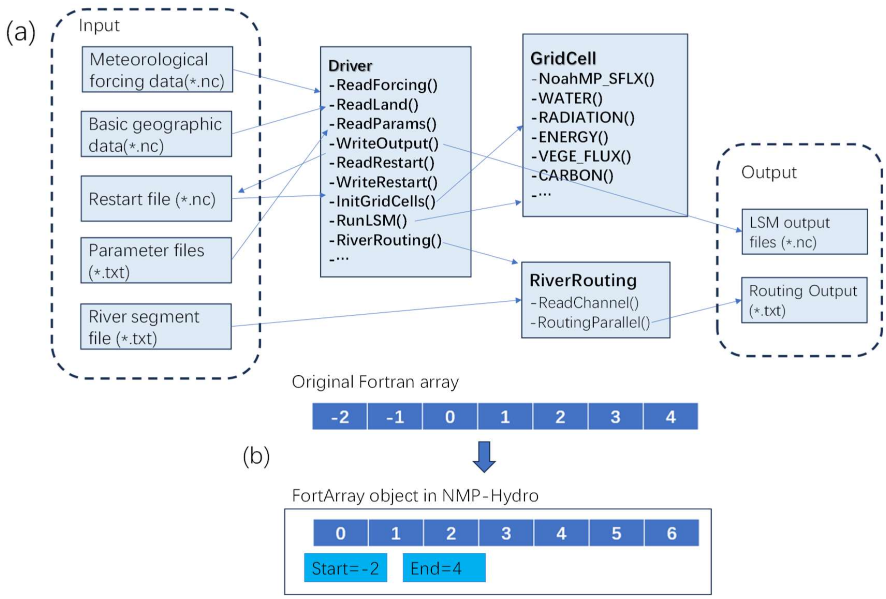

Figure 1. The architectural diagram of NMP-Hydro (a) and the conversion of FORTRAN arrays to C# arrays (b) are depicted in the schematic.

3.2 Coupling with a parallel river routing module

In the development of NMP-Hydro, we integrated a parallel river routing module based on the Muskingum method (Liu et al., 2023), deviating from the previous utilization of the coupled RAPID model in WRF-Hydro (Lin et al., 2018). This parallel river routing module, implemented using C#, incorporates our unique techniques:

1) An array-based sequential processing method for Muskingum routing.
2) A straightforward equal-sized domain decomposition method.
3) Three distinct parallelization schemes for river routing.
4) A specific sorting approach for river segments used in domain decomposition.

This approach's primary advantage lies in its ability to straightforwardly decompose any river network into multiple domains with an equal number of river segments. Achieved by evenly dividing the river segment list into any number of blocks, this innovation capitalizes on the inherent tree-like structure present in most river networks. Importantly, it does not necessitate consideration of the topological conditions specific to a given network, as required in studies such as Mizukami et al. (2021) or David et al. (2015). This design allows parallel execution of river routing on modern personal computers equipped with multi-CPU cores.

The integration of the river routing module with the Noah-MP LSM involves assigning lateral inflows from the LSM-simulated total runoff to the river routing model. In the present NMP-Hydro configuration, we utilize a straightforward catchment centroid-based coupling interface (David et al., 2015). This method designates the LSM grid cell containing the catchment centroid (referred to as the "centroid cell") as the location for a river reach to receive lateral inflows. At a specific temporal step, the computed contributing runoff discharge Q_{lat} (unit: m^3/s) is determined by the following expression:

$$Q_{lat} = R(nx, ny) \times F \times 1000$$

https://doi.org/10.5194/gmd-2024-168
Preprint. Discussion started: 10 October 2024

where $R(nx, ny)$ is the runoff (mm, surface + subsurface) simulated by the LSM during the time step, F is the catchment area (km^2) contributing water to the current river segment.
Alternatively, employing weighted assignments from different grid boxes, akin to the method utilized in (Lin et al., 2018), is also a valid approach. However, this method requires the generation of weights from multiple grid boxes. Given the size of each grid box (equivalent to the resolution of meteorological data, typically ranging from 25 km to 100 km), and considering that each grid box can encompass the catchment areas of multiple river segments, the coupling approach using area weighting is unlikely to yield substantial improvements for most river segments.

3.3 Code Debugging Process

To eliminate any potential code errors resulting from incorrect translation, we conducted a thorough review of the code by performing model execution benchmark on a grid domain. These tests were carried out in three stages. Initially, the code underwent a meticulous step-by-step check by examining the printed values of each variable in WRF-Hydro 3.0 running for specific single grid boxes. This debugging process was also conducted on each option of multiple physical parameterization schemes. This process effectively eliminated any code errors arising from inaccurate translation. However, it is important to note that these tests are only feasible for a limited number of temporal steps and grid boxes. Debugging the code through years-long simulations across the entire domain is impractical.
In the second phase, we compared the spatial distribution of multiple state variables and the long-term discharge hydrograph produced at the main river sections by NMP-Hydro with that produced by WRF-Hydro 3.0. After identifying and correcting any erroneous code, the final results indicated that the two models are capable of generating broadly identical outcomes.

4. Benchmark Testing of NMP-Hydro

4.1 Application area and data

4.1.1 Application area

The Yellow River Basin in Northern China is used as a test area of NMP-Hydro. The gridded domain, as illustrated in **Fig.2** and **Fig.3**, encompasses the entirety of the Yellow River Basin (YRB) and the most part of North China, consisting of 350 columns and 170 rows, featuring a resolution of 6 km in Lambert conformal conic projection coordinates. Geophysical information essential for the domain, including digital elevation, land use and land cover, and green vegetation fraction, was extracted from the WRF/WPS 3.5 input database.

https://doi.org/10.5194/gmd-2024-168
Preprint. Discussion started: 10 October 2024

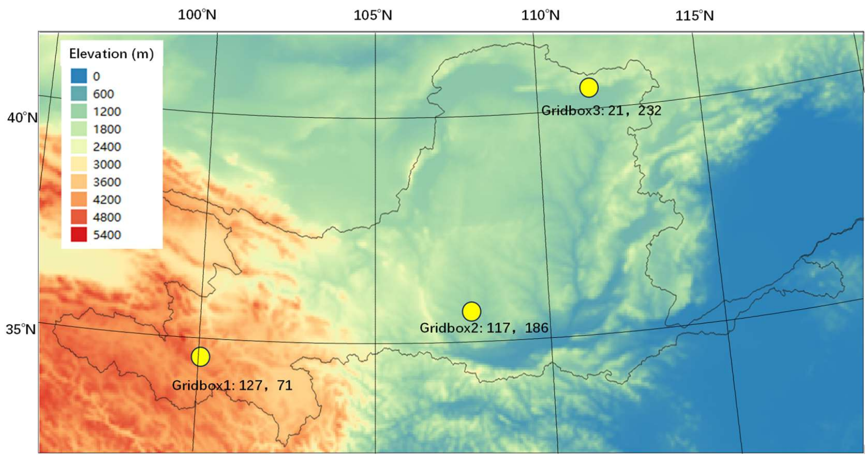

Figure 2. The terrain map of the simulation domain and the three grid boxes for comparison of state variable time series. The three grid boxes are represented by yellow dots, marked with grid box code, the row number and the column rows

For the river routing simulation, the digital river network of the Yellow River was obtained from the HydroSHEDS dataset (version 1) (http://hydrosheds.cr.usgs.gov/). HydroSHEDS is derived from gridded digital elevation data with a resolution of 15 arc-seconds. Given the substantial human intervention and the intricate nature of reproducing observed daily or hourly water discharge, uniform values were assigned to all river segments for the river routing parameters (specifically, the wave celerity (ck) and another parameter (x) describing the river channel condition, as detailed in (David et al., 2013)). No precise calibration is required, as monthly or annual river discharge remains unaffected by changes in routing parameters.

The Yellow River basin experiences significant human impacts, including irrigation, industrial water usage, and groundwater extraction. Major artificial reservoirs and numerous smaller reservoirs regulate the river's discharge, serving as the primary water resource during the dry season. However, such extensive human interference presents substantial challenges in accurately modeling river discharge. Comparatively, the river discharge upstream of the Lanzhou (In Zone 1 as shown Fig.2) hydrological station contributes over half of the entire YRB's total discharge, and is relatively less impacted by dams, enabling us to objectively test the model’s performance.

https://doi.org/10.5194/gmd-2024-168
Preprint. Discussion started: 10 October 2024

Geoscientific Model Development Discussions

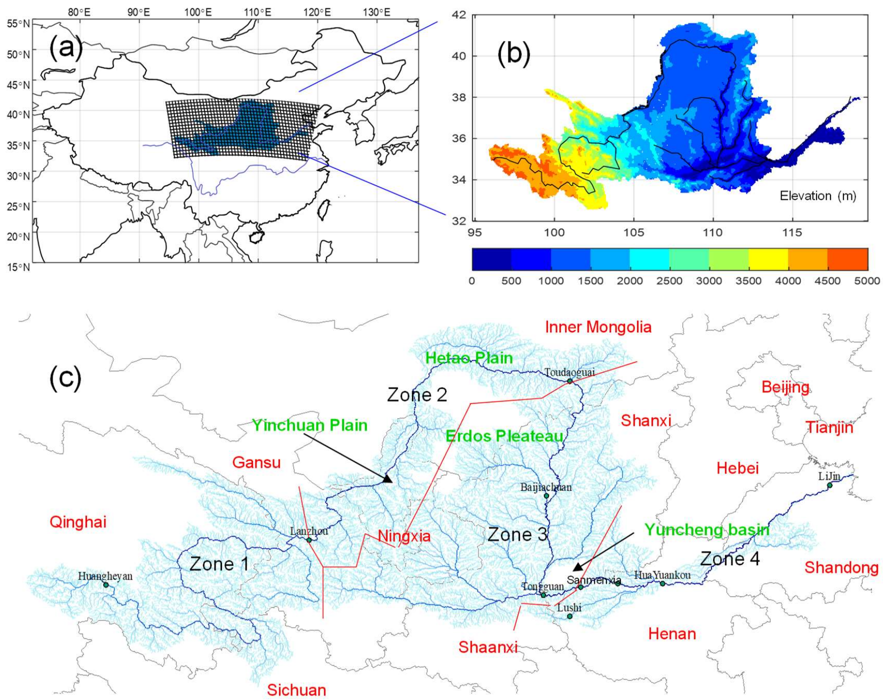

Figure 3. The grid domain covering the Yellow River Basin and the North China area: (a) Geographical location within China; (b) Elevations; (c) Vector River networks utilized for river routing modeling (extracted from the HydroSHEDS dataset). The delineation of the boundaries between distinct zones controlled by four gauging stations (Lanzhou, Toudaoguai, Sanmenxia, Lijin) is represented by red lines.

4.1.2 Meteorological dataset and river discharge data

To drive the model, a 3-hourly meteorological forcing dataset comprising of shortwave and longwave downward radiation, wind velocity, air temperature, relative humidity, air pressure at the surface, and precipitation rate was acquired. The dataset was extracted from the 1.0°×1.0° GLDAS-1 land surface product (Gan et al., 2019; Rodell et al., 2004), for the period 2000-2016. Given the limited availability of observational/reconstructed data between 2001 and 2016, the extracted data pertains to this period, and additional data between 1996 and 2000 was also extracted for the model's spinning-up.

In previous research, the spinning-up of Noah-MP requires 50 years (Wu et al., 2021) or more than one hundred years (Zheng et al., 2019) to achieve an equilibrium state. However, in this study, the spin-up process was conducted in two steps. In the first step, the period from 1996 to 2016 was run three times to generate a 'restart file' for a 63-year spinning-up, utilizing the initial PS combination (11131-2222-121). In the second step, starting from this initial combination, new schemes were introduced, and the 'restart file' was used to initiate the formal experiments covering the period from 1996 to 2016.

The dataset of Natural River Discharge (RND) reconstructed by the Yellow River Conservancy Commission of the Ministry of Water Resources was gathered to assess the model output. Annual natural discharges from the monitoring station of Lanzhou were collected for the period from 2001 to 2016.

https://doi.org/10.5194/gmd-2024-168
Preprint. Discussion started: 10 October 2024

4.2 Comparing the outputs of NMP-Hydro and WRF-Hydro3.0

It is noteworthy that there are numerous parameterization scheme combinations for Noah-MP, which makes it unfeasible to compare the results generated under all scheme combinations. Therefore, the output of NMP-Hydro and WRF-Hydro under the default parameterization scheme combination was compared, based on the exact same meteorological dataset. The comparison was conducted in two ways. The first comparison is that of the spatial maps of multiple variables (Table 2) for a specific year or day. For each state variable, such as SFCRNOFF, the maps of state variables simulated by NMP-Hydro and WRF-Hydro are presented. The difference (⊿) between the values of the same variables simulated by the two 'Noah-MP models' is calculated as

$\varDelta = V_{\text{NMP-Hydro}} - V_{\text{WRF-Hydro}}$

Where $V_{\text{NMP-Hydro}}$ and $V_{\text{WRF-Hydro}}$ are the state variable simulated by the two Noah-MP models, respectively. For certain variables, such as SFCRNOFF, UGDRNOFF, ECAN and ETRAN, the percentive relative differences were also calculated as follows:

$\delta = 100 \cdot \Delta / V\text{WRF-Hydro}$

The second method is to compare the variations of state variables at specific grid boxes. In this case, only three grid boxes (Fig. 2) were selected to extract the state variable time series.

Table 2 The state variables simulated by NMP-Hydro and WRF-Hydro, which is verified by generating maps

Variable name	description	unit
SFCRNOFF	Accumulated Surface runoff	mm
UGDRNOFF	Accumulated ground runoff	mm
ECAN	Evaporation from canopy	mm
ETRAN	Vegetation transpiration	mm
TV	Vegetation temperature	K
TG	Ground temperature	K
EAH	Canopy air vapor pressure	Pa
EVG	Ground evaporation heat	W/m^2
CHV	Exchange coefficient vegetated	m/s
CHLEAF		
TR	Transpiration heat	W/m^2
EVB	Evaporation heat to atmosphere bare	W/m^2
FIRA	Total net long-wave radiation to atmosphere	W/m^2
TRAD	Surface radiative temperature	K
ALBEDO	Surface albedo	--

4.2.1 Maps of state variables simulated

To test whether NMP-Hydro can produce the corresponding outputs of the original WRF-Hydro (Fortran-version Noah-MP), many state variables (Table 3) from multiple time slices (10 June 2000, 10 June 2001, 10 June 2004, and 10 June 2008) were checked by drawing maps. The maps for two representative

https://doi.org/10.5194/gmd-2024-168
Preprint. Discussion started: 10 October 2024

variables (SFCRNOFF and TV) are shown in Fig.4 and Fig.6. As can be seen, there is visually little difference in the spatial patterns of the results. Similarly, no discernable visual difference is also apparent for the maps of other variables. However, the relative difference of annual surface runoff and annual underground runoff is significant large at some areas (generally in high-elevation regions), where NMP-Hydro underestimated those values by 10%~30% (**Fig.4**). Generally, the difference in TV is smaller than 0.2 ℃, but in some sporadically districted locations, the TV's difference can be larger than 2 ℃ (**Fig.6**).

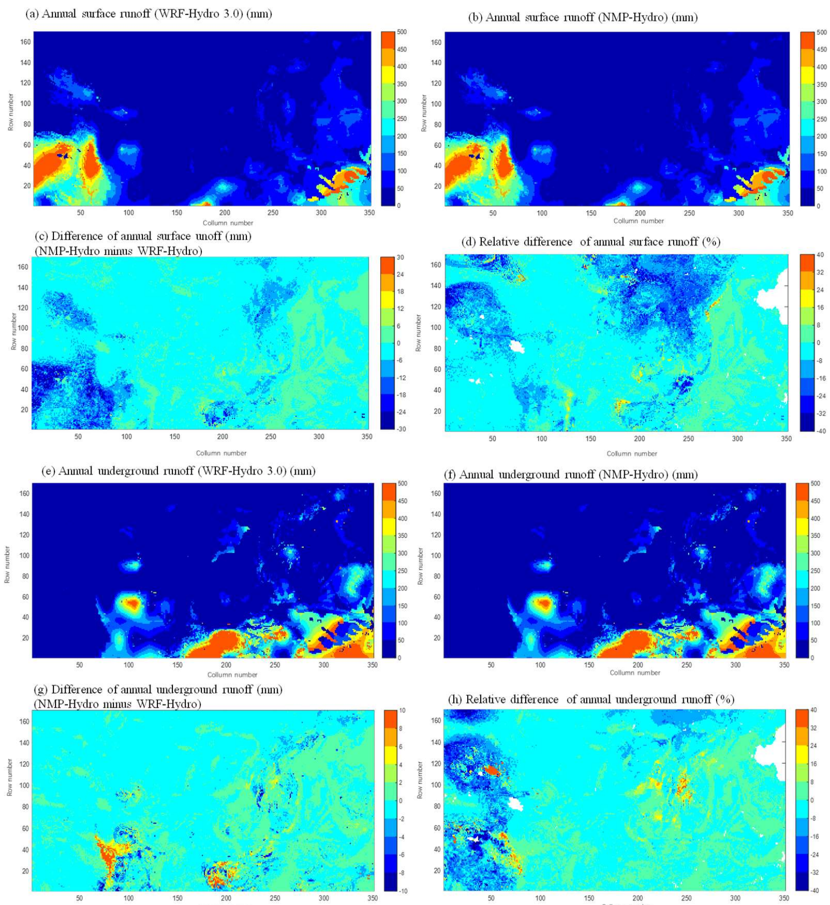

Figure 4. Maps of annual total values, differences, and relative differences of SFCRNOFF (surface runoff, mm) and UGDRNOFF (underground runoff, mm) simulated by WRF-Hydro3.0 and NMP-Hydro 1.0, for the year 2005.

The monthly temporal variations of three representative grid boxes (as shown in **Fig.2**) indicate that the two models produced consistent changes (**Fig.8**). For certain variables, SFCRNOFF、TG、FIRA、CHV, occasionally, some significant differences was found in certain months for Gridbox2. It is such occasionally happened differences that caused the spatial disparity as shown in **Fig.4-5**. We checked the disparity at certain grid boxes on the daily scale and found that the differences also happen sporadically (**Fig.5**). Most of the differences occur during the cold months (November, December, January, and

https://doi.org/10.5194/gmd-2024-168
Preprint. Discussion started: 10 October 2024

February). However, it is worth noting that most of the simulated SFCRNOFF in these months show no difference, and this difference is also independent of whether precipitation occurred during these days. Each difference is caused by a mismatch in the simulated peak time (**Fig.5**), manifested as a one-day lag effect of NMP-Hydro relative to WRF-Hydro. Meanwhile, this lag effect of NMP-Hydro also causes underestimated or overestimated total surface runoff. Considering such mismatch usually happens in cold months and high-elevation regions, it may be caused by the different calculation accuracy for the processes of ice, snow and frozen soil. Although the code for these processes in Noah-MP is complex enough, we have checked the code multiple times and have not found any coding difference, so these differences are likely the result of floating-point errors.

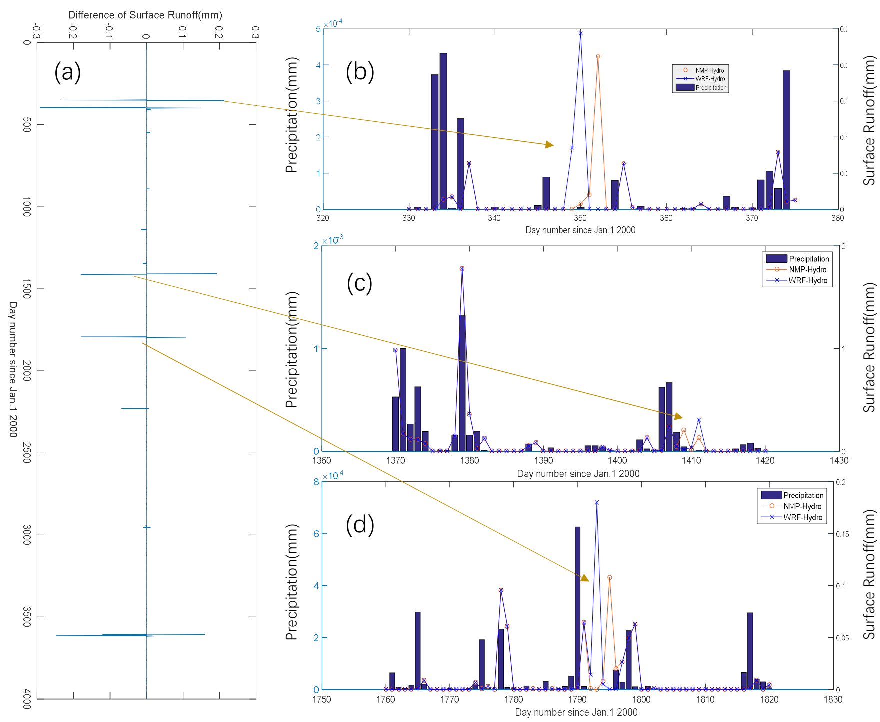

Figure 5. Simulated difference in daily surface runoff (SFCRNOFF) series simulated by NMP-Hydro and WRF-Hydro for Gridbox3. (a) the SFCRNOFF difference of NMP-Hydro to WRF-Hydro; (b-c) the disparities of SFCRNOFF near the day number 350, 1410 and 1790, respectively.

Given these discrepancies on a monthly scale, no NSE smaller than 0.9 and correlations smaller than 0.98 were identified. For the three representative grid boxes, no significant differences were identified for certain variables, including TR, EAH, TV, ACCETRAN, UGDRNOFF, and others (**Fig.8**). The daily time series from Gridbox3 are extracted, then are compared between the NMP-Hydro and the WRF-Hydro. It is evident that EDIR, SFCRNOFF, soil water content and TV exhibit smaller discrepancies, whereas TG and ALBEDO demonstrate larger disparities (**Fig.7**). The discrepancies are pronounced when TG and TV below zero.

The reason for occasional discrepancies between the outputs of two models remains elusive, as it is challenging to ascertain through the process of code checking and debugging. Such discrepancies may

https://doi.org/10.5194/gmd-2024-168
Preprint. Discussion started: 10 October 2024

be attributed to a number of factors, including floating-point calculation errors, disparate parameter configurations, or encoding inconsistencies. The former two are reasonable and acceptable, whereas a coding mismatch is typically unacceptable. Nevertheless, identifying discrepancies is only feasible during the initial stages of debugging, but not for tens to hundreds of subsequent iterations. It is not uncommon for errors to remain undetected even after the execution of numerous time steps. In this study, in light of the fact that no inconsistencies remained after checking the code many times, it is plausible that floating-point errors play a significant role in explaining the discrepancies. During the debugging process, we found inconsistency always arise from the recursive calculation of energy transferring for vegetated and bare land, such as variables TV and TG. The floating-point error of temperature could potentially result in markedly divergent outcomes during transitions around frozen temperature.

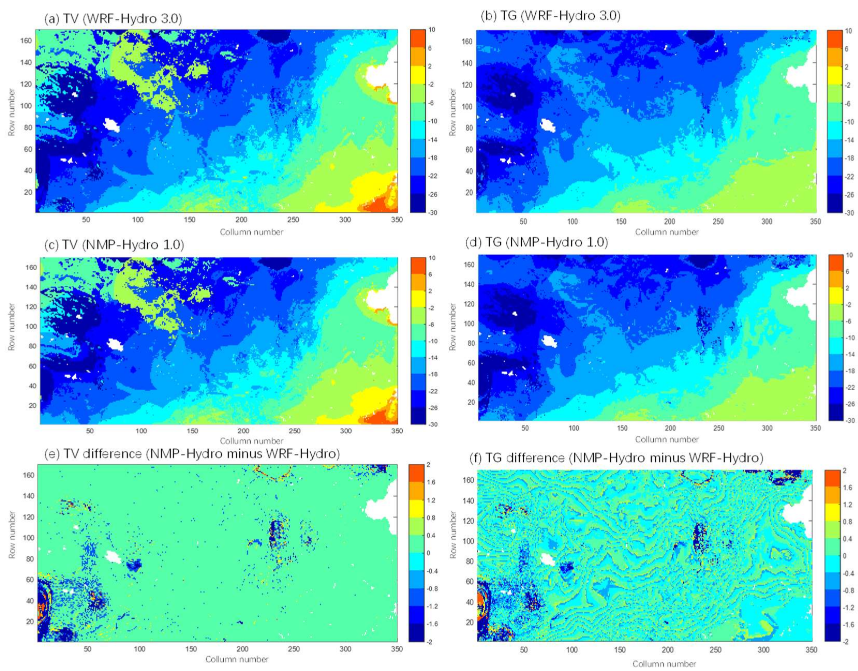

Figure 6: Maps of TV (vegetation temperature, K) and TG (ground temperature, ˚C) simulated by WRF-Hydro3.0 and NMP-Hydro 1.0, for the day Jan. 1st, 2008

https://doi.org/10.5194/gmd-2024-168
Preprint. Discussion started: 10 October 2024

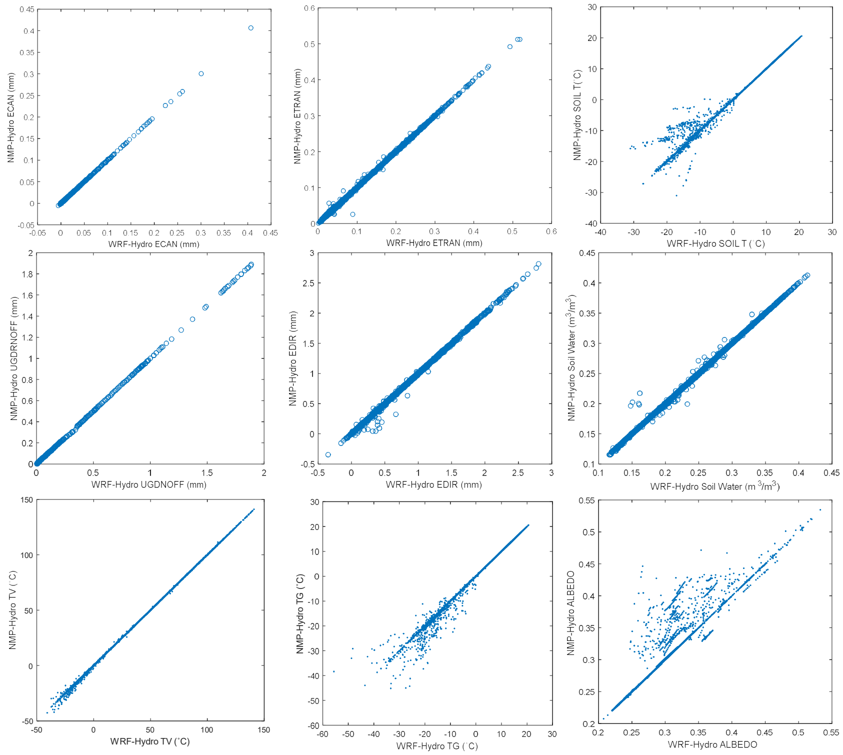

Figure 7. Daily state variables simulated by NMP-Hydro versus by WRF-Hydro at Gridbox3

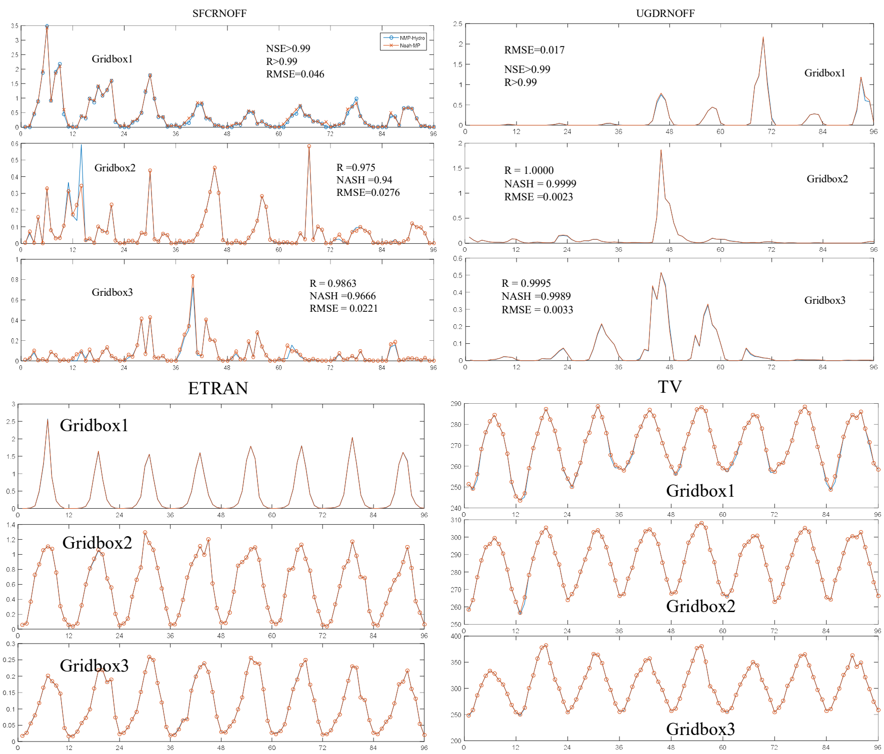

Figure 8: Monthly surface runoff (mm), underground runoff(mm), transpiration (mm) and vegetation temperature (K) simulated by WRF-Hydro3.0(Noah-MP, blue) and NMP-Hydro (red) at the three grid boxes, 2000-2007.

4.3 Streamflow discharges simulated by multiple experiments

4.3.1 Experimental design of Noah-MP simulation

Here, we present the numerical outputs of NMP-Hydro and the comparison with WRF-Hydro/Noah-MP. The parallel speedup of NMP-Hydro will not be evaluated here, as it is a straightforward implementation in C# for executing multiple tasks. The description of parallelization of the coupled river routing models has been clearly described in our previous publication(Liu et al., 2023).

To verify whether the various parameterization schemes (PSs) of NMP-Hydro can produce reasonable discharge for the Yellow River catchment area, this study conducted 17 Noah-MP simulations using different PS combinations. Given the challenge of determining the relative importance of each parameterization and the impracticality of including all possible combinations, we adopted a strategic approach. A fixed PS combination was established as a foundation, and alterations were made to one parameterization's scheme at a time (refer to Table 3).

In addition to our selected parameterizations, we considered commonly used PS combinations, including the 'default' combination proposed by Noah-MP developers. Sensitivity analysis was conducted by analyzing the differences or variations among these incomplete PS combinations. It is important to note

https://doi.org/10.5194/gmd-2024-168
Preprint. Discussion started: 10 October 2024

that the chosen PS combinations represent only a subset of all possible combinations, and the assumed sensitivities based on this subset are considered indicative of overall sensitivities based on the complete set of combinations.

The PS combinations are represented by codes consisting of sequential digital numbers. For instance, the default combination is denoted as '11131-1132-111', where each number signifies a scheme option. The initial experiment, arbitrarily set as the PS combination of '11131-2222-121', served as the foundation for subsequent experiments. Fifteen experiments (refer to Table 2) were then conducted by modifying one option at a time from the initial experiment.

These experiments are categorized into multiple groups, with the initial experiment '11131-2222-121' being employed in multiple groups:

Runoff scheme group (four experiments, switching between: 1. SIMGM, 2. SIMTOP, 3. Schaake96, 4. BATS);

Vegetation scheme group (five experiments, switching between the first option and the fifth option, see Table 1);

β-factor option group (three experiments, switching between Noah, CLM, and SSiB);

Radiation transfer option group (three experiments, switching between three options);

Group for the scheme of the lower boundary of soil temperature (six experiments);

Group for stomatal conductance scheme (two experiments, switching between two options).

Table 3. Experiments conducted in this study

Number	PS combination code	Abbreviated code	Description
1	11131-2222-121	11131 or 11131-222 or 11131*121	The first experiment
2	11111-2222-121	11111	Experiments with RUN
3	11121-2222-121	11121	
4	11141-2222-121	11141	
5	21131-2222-121	21131 or 21131*121	Experiments with DVEG
6	31131-2222-121	31131	
7	41131-2222-121	41131	
8	51131-2222-121	51131 or 51131*121	
9	11231-2222-121	11231	Experiments with BTR
10	11331-2222-121	11331	
11	11131-2212-121	11131-221	Experiments with RAD
12	11131-2232-121	11131-223	
13	12131-2222-121	12131	Experiments with CRS
14	11131-1132-111	'default'	The default PS combination proposed by Noah-MP developers
15	11131-2222-111	11131*111	Experiments with TBOT
16	21131-2222-111	21131*111	
17	51131-2222-111	51131*111	

4.3.2 Simulated streamflow under various parameterization schemes

We simply use the Taylor diagram (Taylor, 2001) to evaluate the different PS on the river discharge at the Lanzhou station. Taylor diagram provides a graphical representation of a model's simulation performance, encompassing three key indices: correlation coefficient (R), root-mean-square error (RMSE), and standard deviation (SD).

The streamflow discharges were produced by coupling the NMP-Hydro with the parallel river routing model. The results showed that, in general, the various scheme combinations of parameterizations can produce monthly river discharge close to the result of the original Noah-MP (WRF-Hydro) for the Lanzhou station. A preliminary comparison on the various scheme combinations is presented in **Table 4**. The monthly performance is summarized in Table 4 based on the comparison of the different PSs as shown in **Fig. 9**. It can be observed that for the majority of parameterizations, the discharges in winter are not sensitive to the schemes, this is to be expected, given the minimal runoff during this season. The simulated summer discharges exhibit notable degree of sensitivity with regard to the various parametrization schemes. In relation to the runoff parametrization, the results obtained through the utilization of the SIGGM scheme led to overestimation during the winter season and underestimation during summer, signifying that considering groundwater could enhance the simulation accuracy of the catchment modulation as opposed to other schemes.

For the Lanzhou station, over 50% of experiments produced discharges with correlations larger than 0.9 (Fig.10). The PS combination '11141-2222-121' yielded the highest correlation, and '11131-2222-111' showed the highest performance according to Taylor's score.

https://doi.org/10.5194/gmd-2024-168
Preprint. Discussion started: 10 October 2024

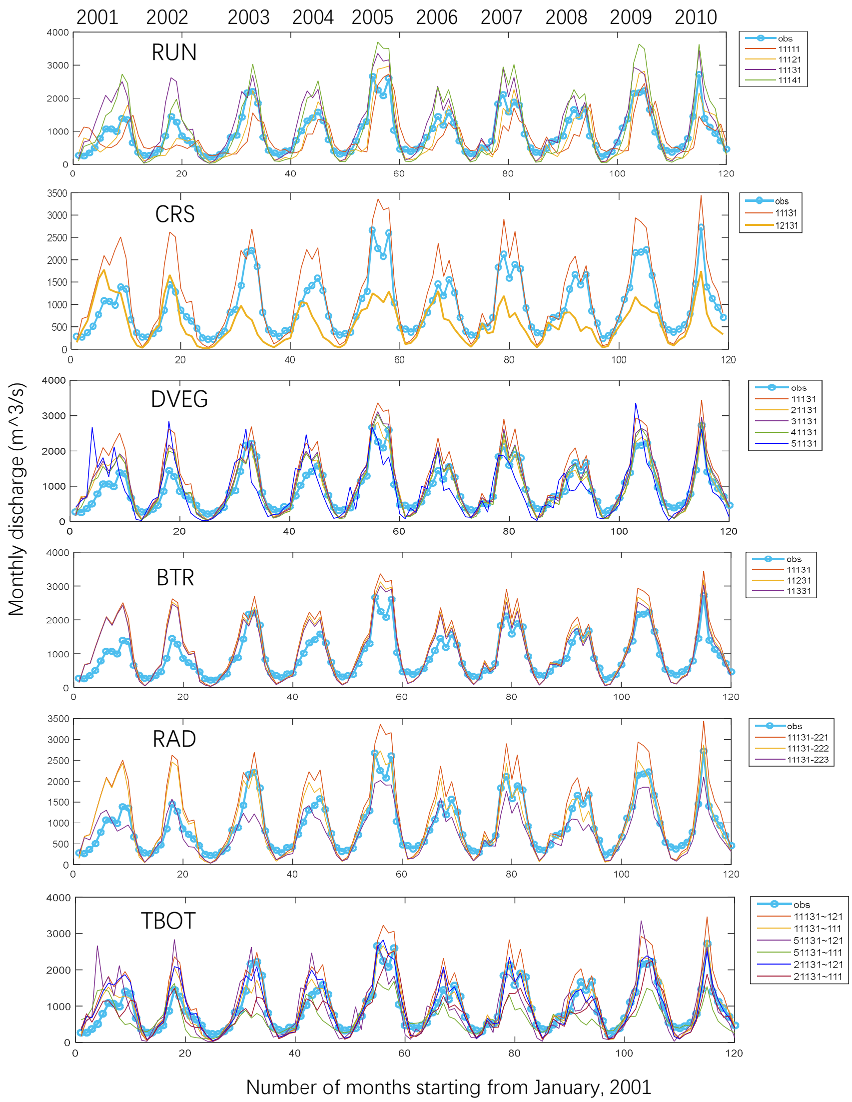

Figure 9: Monthly River discharge (m^3/s) for Lanzhou. The first subplot displays the results simulated with varying RUN schemes while the other subplots follow a similar pattern. Reconstructed natural discharge is denoted as 'obs'.

https://doi.org/10.5194/gmd-2024-168
Preprint. Discussion started: 10 October 2024

Geoscientific Model Development
Discussions
Open Access
EGU

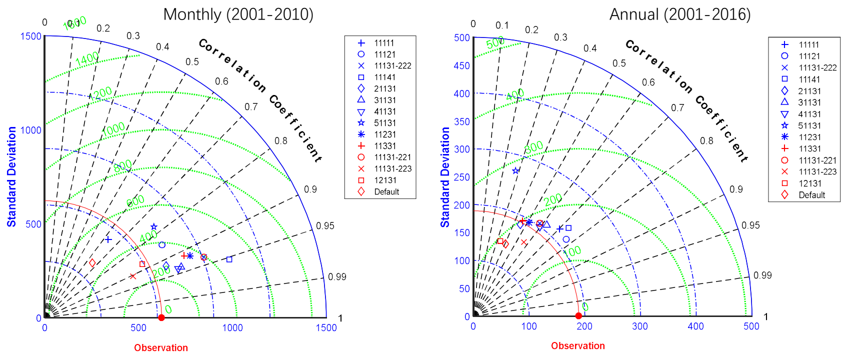

Figure 10: Taylor diagram for monthly and annual mean river discharge (m^3/s) at the Lanzhou monitoring station

Table 4: Performance of various parameterization schemes on monthly discharge for Lanzhou station

	scheme	Winter	summer
RUN	1.SIGGM	Overestimation	underestimation
	2.SIMTOP	underestimation	Small overestimation
	3.Schaake96		Large overestimation
	4.BATS		The Largest overestimation
CRS	1. Ball-Berry	Small difference	Overestimation
	2. Jarvis		Underestimation
DVEG	1.Table LAI, read FVEG	No significant difference	The largest overestimation
	2.dynamical LAI and FVEG=f(LAI)		Mostly small overestimation
	3. table LAI, FVEG=f(LAI)		
	4 table LAI, FVEG=maximum		
	5.Dynamical LAI, maximum FVEG	Unstable overestimation and underestimation	
BTR	1.Noah	No significant difference	The largest overestimation
	2.CLM		The middle overestimation
	3.SSib		The smallest overestimation
RAD	1. gap=F(3D, cosz)	No significant difference	Large overestimation
	2. gap=0		Slight overestimation
	3. gap=1-FVEG		underestimation
TBOT	1. Zero flux	No significant difference	large
	2.Noah		small

5 Model code and technical documentation for NMP-Hydro

We archive, manage, and maintain the NMP-Hydro at https://github.com/lsucksis/NMP-Hydro for public access. A technical description was provided at the same site.

5 Conclusions

This study presents the NMP-Hydro model, which is a reconstructed land surface eco-hydrological model based on Noah-MP. The model was developed by translating the FORTRAN code of Noah-MP (in WRF-Hydro 3.0) into C# and also coupling it with a river routing model. The model has been designed for parallel execution on Windows systems, thereby capitalizing on the multi-core CPUs that are now a standard feature of personal computers. The NMP-Hydro code has been subjected to rigorous testing to ensure that it produces results that are consistent with those of the original WRF-Hydro. The code is based on the C# language, which facilitates greater user-friendliness and facilitates modification and expansion.

The development of this software enabled the successful execution of high-resolution simulations encompassing a 6-km span within the Yellow River Basin (YRB). These simulations were conducted with a multitude of parameter scheme (PS) combinations within the Noah-MP framework. Maps of all the outputs (runoff, evaporation, groundwater, energy, vegetation) across the grid domain demonstrate consistent spatial patterns that are simulated by the two models. The long-term variations of multiple state variables simulated by the two models also exhibit high consistency, although some differences are evident. Identifying the cause of this simulation discrepancy in the outputs of the two models is a challenging task, given the intricate nature of the Noah-MP code. The sporadic occurrence of errors may be attributed to the accumulation of floating-point numerical calculation errors, especially for the cases below frozen temperature.

With regard to the Lanzhou hydrological station, the river discharge simulated by NMP-Hydro based on the multiple scheme combination of parameterizations is found to be in reasonable agreement with the reconstructed natural river discharge.

Overall, while there are discrepancies in the simulated results when compared to the original model, the NMP-Hydro model reproduces consistent spatiotemporal distribution of multiple variables as that by WRF-Hydro. Given the complex nature of long-term state variables in Noah-MP, which reflect multiple processes including runoff production, energy transfer and dynamical vegetation, the results of NMP-Hydro and WRF-Hydro/Noah-MP remain highly consistent. It can therefore be asserted that NMP-Hydro can be considered a reliable replica of Noah-MP in the uncoupled WRF-Hydro 3.0. It was inevitable that minor modifications to the code or model parameters would be required during the testing phase of NMP-Hydro. This presented a significant challenge in reproducing the identical outputs as those generated by WRF-Hydro.

Acknowledgements. Thanks Pei-Rong Lin for her great efforts in guiding Yong-He Liu through the intricacies of Noah-MP.

Code and data availability. 1. The NMP-Hydro model code is available at https://github.com/lsucksis/NMP-Hydro. 2. The Noah-MP technical documentation is available at the same site and more details will continue to be added in the documentation. 3. The benchmark meteorological datasets for driving NMP-Hydro and WRF-Hydro 3.0 were uploaded to the Science Data Bank (DOI: https://doi.org/10.57760/sciencedb.13122).

Author contributions. Yong-He Liu has translated the code of WRF-Hydro/Noah-MP to NMP-Hydro, the debugging and the benchmark model simulations. The work is led by Zong-Liang Yang. Liu has drafted the paper, with improvement made by Yang.

Competing interests. The contact author has declared that none of the authors has any competing interests

Financial support. This work is funded by the Project on the Creation of "Double First-class" Disciplines in Surveying and Mapping Science and Technology (Grant No. GCCYJ202418), Henan Polytechnic University.

References

Bales, J., 2019. Featured Collection Introduction: National Water Model II. J. Am. Water Resour. As., 55(4): 938-939, https://doi.org/10.1111/1752-1688.12786.

Chang, M. et al., 2020. An optimal ensemble of the Noah-MP land surface model for simulating surface heat fluxes over a typical subtropical forest in South China. Agr. Forest Meteorol., 281, https://doi.org/10.1016/j.agrformet.2019.107815.

Chen, F. et al., 2007. Description and evaluation of the characteristics of the NCAR high-resolution land data assimilation system. J. Appl Meteorol Clim, 46(6): 694-713, https://doi.org/10.1175/JAM2463.1.

Francesca, V. et al., 2020. A Multiscale, Hydrometeorological Forecast Evaluation of National Water Model Forecasts of the May 2018 Ellicott City, Maryland, Flood. J. Hydrometeorol., 21(3).

Gan, Y. et al., 2019. Assessment and Reduction of the Physical Parameterization Uncertainty for Noah-MP Land Surface Model. Water Resour. Res., 55(7): 5518-5538, https://doi.org/10.1029/2019WR024814.

Gao, Y., Li, K., Chen, F., Jiang, Y. and Lu, C., 2015. Assessing and improving Noah-MP land model simulations for the central Tibetan Plateau. J. Geophys. Res.-Atmos., 120(18): 9258-9278, https://doi.org/10.1002/2015JD023404.

Gochis, D.J.A.C., 2020. The WRF-Hydro modeling system technical description (version 5.1.1). NCAR Tech. Note.

He, C. et al., 2023. Modernizing the open-source community Noah with multi-parameterization options (Noah-MP) land surface model (version 5.0) with enhanced modularity, interoperability, and applicability. Geosci Model Dev, 16(17): 5131-5151, https://doi.org/10.5194/gmd-16-5131-2023.

Karki, R., Krienert, J.M., Hong, M. and Steward, D.R., 2021. Evaluating Baseflow Simulation in the National Water Model: A Case Study in the Northern High Plains Region, USA. J. Am. Water Resour. As., 57(2): 267-280, https://doi.org/10.1111/1752-1688.12911.

Li, J. et al., 2022. Global Evaluation of the Noah-MP Land Surface Model and Suggestions for Selecting Parameterization Schemes. J. Geophys. Res.-Atmos., 127(5), https://doi.org/10.1029/2021JD035753.

Liang, X., Lettenmaier, D.P., Wood, E.F. and Burges, S.J., 1994. A simple hydrologically based model of land surface water and energy fluxes for general circulation models. Journal of Geophysical Research: Atmospheres, 99(D7).

Lin, P. et al., 2018. Implementation of a vector-based river network routing scheme in the community WRF-Hydro modeling framework for flood discharge simulation. Environ. Modell. Softw., 107: 1-11, https://doi.org/10.1016/j.envsoft.2018.05.018.

Liu, Y., Yang, Z. and Lin, P., 2023. Parallel river channel routing computation based on a straightforward domain decomposition of river networks. J. Hydrol., 625, https://doi.org/10.1016/j.jhydrol.2023.129988.

Ma, N. et al., 2017. A Systematic Evaluation of Noah-MP in Simulating Land-Atmosphere Energy, Water, and Carbon Exchanges Over the Continental United States. J. Geophys. Res.-Atmos., 122(22): 12245-12268, https://doi.org/10.1002/2017JD027597.

Niu, G. et al., 2011. The community Noah land surface model with multiparameterization options (Noah-MP): 1. Model description and evaluation with local-scale measurements. J. Geophys. Res.-Atmos., 116(D12109), https://doi.org/10.1029/2010JD015139.

Rodell, M., Houser, P.R., Jambor, U., Gottschalck, J. and Mitchell, K., 2004. The global land data assimilation system. B. Am. Meteorol. Soc., 85(3): 381-394.

Taylor, K.E., 2001. Summarizing multiple aspects of model performance in a single diagram. Journal of Geophysical Research: Atmospheres, 106(D7): 7183-7192, https://doi.org/https://doi.org/10.1029/2000JD900719.

Wu, W., Yang, Z. and Barlage, M., 2021. The Impact of Noah-MP Physical Parameterizations on Modeling Water Availability during Droughts in the Texas-Gulf Region. J. Hydrometeorol., 22(5): 1221-1233, https://doi.org/10.1175/JHM-D-20-0189.1.

Yang, Q. et al., 2021. Quantitative assessment of the parameterization sensitivity of the Noah-MP land surface model with dynamic vegetation using ChinaFLUX data. Agr. Forest Meteorol., 307, https://doi.org/10.1016/j.agrformet.2021.108542.

Yang, Z. et al., 2011. The community Noah land surface model with multiparameterization options (Noah-MP): 2. Evaluation over global river basins. J. Geophys. Res.-Atmos., 116(D12110), https://doi.org/10.1029/2010JD015140.

Zheng, H. et al., 2019. On the Sensitivity of the Precipitation Partitioning Into Evapotranspiration and Runoff in Land Surface Parameterizations. Water Resour. Res., 55(1): 95-111, https://doi.org/10.1029/2017WR022236.